

Boundary Distribution Estimation to Precise Object Detection

Haoran Zhou
zhouhr19@lzu.edu.cn

Hang Huang
huangh2018@lzu.edu.cn

Rui Zhao
zhaor19@lzu.edu.cn

Wei Wang
wangw2019@lzu.edu.cn

Qingguo Zhou*
zhouqg@lzu.edu.cn

School of Information Science &
Engineering
Lanzhou University
Lanzhou, China

Abstract

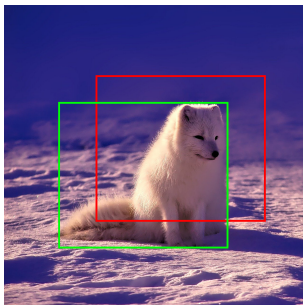
In principal modern detectors, the task of object localization is implemented by the box subnet which concentrates on bounding box regression. The box subnet customarily predicts the position of the object by regressing box center position and scaling factors. Although this approach is frequently adopted, we observe that the result of localization remains defective, which makes the performance of the detector unsatisfactory. In this paper, we prove the flaws in the previous method through theoretical analysis and experimental verification and propose a novel solution to detect objects precisely. Rather than plainly focusing on center and size, our approach refines the edges of the bounding box on previous localization results by estimating the distribution at the boundary of the object. Experimental results have shown the potentiality and generalization of our proposed method.

1 Introduction

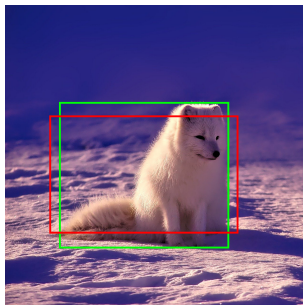
As the combination of classification and localization, object detection is intended to spot desired objects in the image and categorize them respectively. The task of object classification has been pushed forward substantially in recent years by virtue of the development of deep learning frameworks. Classifiers [35, 38, 39] are now able to achieve convincing grades on various challenging benchmarks [32, 33, 36]. However, the result of localization remains unsatisfactory and limits the overall detection performance as a result.

In principal modern detectors, *e.g.*, *Faster R-CNN* [34], *RetinaNet* [26], and *CenterNet* [24], the task of object localization is implemented by the box subnet which concentrates on bounding box regression. The box subnet customarily predicts bounding boxes by regressing box center position (x, y) and the scaling factors (w, h). Although has shown effective

results in previous state-of-the-art frameworks, this design has inherent defects for precise localization. As shown in Figure 1, each variable of (x, y, w, h) affects multiple edges when adjusting the center position or the size of the box. As a result, all edges of the box shift as a whole. Besides, the center-focus representation method induces an imbalance of features, *i.e.*, detectors pay more attention to internal features that are less important for localization.



(a) Center tuning



(b) Size tuning

Figure 1: Illustration of the center-size box tuning method. The **Green** box represents the ground truth. The **Red** box represents the prediction box with center error or size error only.

The purpose of precise localization is to bridge the gap between prediction and ground truth. For humans, the most efficient way to annotate ground truth boxes is by individually aligning each side of the box with the corresponding boundary. Inspired by the manual annotation method, we propose a novel solution for precise localization by refining previous localization results with estimations of actual boundary distribution. It first predicts the boundary on the proposed area of the previous pipeline. The coarse boundary is then determined from the boundary possibility map. For each side of the box, the corresponding fine boundary distribution is estimated based on the coarse boundary context and used to refine the final results.

We deploy the proposed method on multiple frameworks and evaluate them on the MS COCO dataset [25]. Our method shows potentiality with plain functional estimation. Specifically, an improvement of 2.0% AP is achieved without extra annotation data on the competent *Mask R-CNN* [16] baseline.

Our main contributions can be summarized as follows:

- We introduce our universal precise object detection method which refines the edges of the bounding box on previous localization result by estimating the boundary distribution of the object.
- To precisely generate each side of bounding box, we evaluate different representation methods of the bounding box and believe that the edge representation method is more appropriate for precise localization.
- To leverage boundary features, we devise coarse-to-fine boundary distribution estimation modules, which achieve a significant improvement compared to previous cascade architectures.

2 Related Work

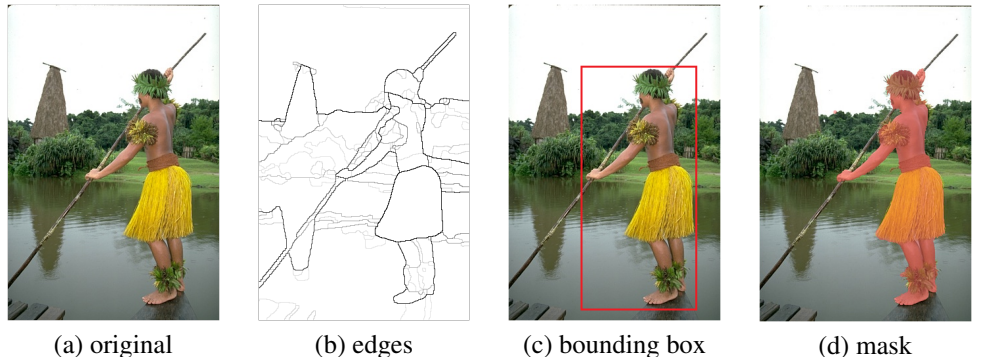


Figure 2: Illustration of some boundary-related applications in computer vision (edge detection, object detection, and instance segmentation).

2.1 Localization in Detection

As a result of the dramatic development of deep learning in recent years, CNN-based methods progressively become the dominant solutions in detection applications. Deep learning detectors can be basically divided into three categories by different structures: two-stage detectors [8, 13, 14, 16, 29, 32], one-stage detectors [28, 30, 33], and anchor-free detectors [40, 42].

Although different in implementation, these methods all follow the classification-localization paradigm. Fundamentally, four independent variables are required to represent a bounding box. In anchor-based detectors, *e.g.*, *Faster R-CNN* [34] and *RetinaNet* [26], the bounding box is regressed from the proposal or pre-defined anchor and represented as the format of the offsets of the center (δ_x, δ_y) and the relative scaling factors (δ_w, δ_h). Anchor-free methods such as *FCOS* [40] and *CenterNet* [44] similarly predict the center of the object and the corresponding size. These center-size box tuning methods are able to locate objects efficiently but are subject to inevitable errors. To eliminate the error, *CornerNet* [23] introduces a novel method to use the object’s top-left corner and bottom-right corner to compose the bounding box. However, it imports extra computational cost by grouping corner pairs. Our method combines the advantages of the two methods through refining edges on previous localization results.

2.2 Boundary in Computer Vision

It has been long understood that edges and boundaries are often defined to be semantically meaningful in tasks at different levels. Among various types of other related applications in computer vision, we briefly introduce two representative applications to illustrate the similarities and differences between our method and theirs.

Edge detection, considered as a low-level task, aims to extract visually salient edges and object boundaries from nature images. Generally speaking, it can be divided into three categories: early filter methods [9, 10, 11, 12], information theory methods [1, 2, 3],

learning-based methods [8, 9, 14, 15]. Recent CNN-based methods [10, 11, 12, 13, 16] try to learn hierarchical features automatically. However, they still struggle to distinguish object boundaries from detection results. It is difficult to complete object-level tasks with these low-level cues of edges.

Instance segmentation aims to give dense inference by generating pixel-wise masks. It gives different labels for separate instances of objects belonging to the same class. Some of these methods [6, 7, 16, 17, 18] work based on existing detectors. They first use the detector to obtain proposals, then predict masks on these areas. However, these methods require pixel-level annotation, which is often not available in the detection scene.

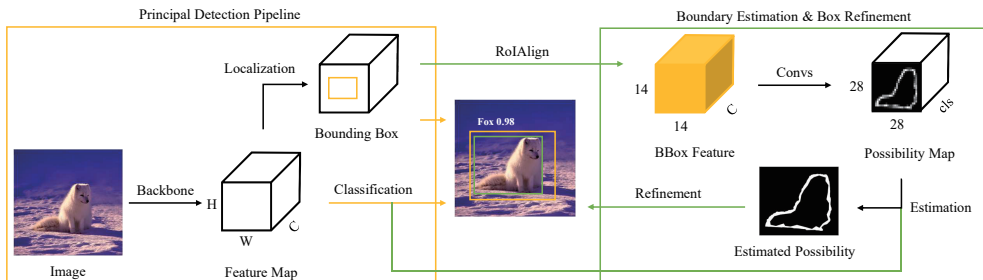


Figure 3: Illustration of principal detection pipelines with boundary estimation and box refinement. The result of the detector is further used to crop and resize corresponding box features, segment the boundary in the bounding box. The object bounding box is finally refined with the estimated boundary.

2.3 Detection with Boundary Features

Boundary context such as surroundings and the shape of the object contains valuable information for detection applications. Traditional detectors, *e.g.*, *Sobel* [11], *Canny* [12], *Marr-Hildreth* [13], usually leverage smoothing filters or image gradients to extract local features in low level. *Edge Boxes* [14] introduces a proposal algorithm based on edges in the input image. It works fine with a single object but struggles to divide multiple objects. These image-based detectors are flawed in some ways, as they merely take the low-level visual context of objects, and hard to apply on modern detectors. *Deformable R-FCN* [10] uses deformable convolution to include context information. *BAN* [15] proposes a boundary-aware network to leverage boundary context. *SABL* [16] tries to predict precise object boundary with buckets. We refer to these deep-learning-based methods and devise our estimation module to leverage boundary context of the object.

3 Method

In this work, we focus on improving the localization module in modern detectors. Inspired by the manual annotation method, we select edge-focus box representation as the key to precise localization and devise a novel boundary estimation method to leverage boundary features. The whole pipeline works as shown in Figure 3.

Our proposed method follows the principal detection pipeline which regards object detection as a combination of localization and classification. Features of the object are cropped

and resized based on previous localization results. They are then used to predict the coarse boundary, and further estimate the fine boundary. Each side of the box is refined with a corresponding estimated fine boundary. Our method does not rely on a specific detection pipeline and needs no extra annotation.

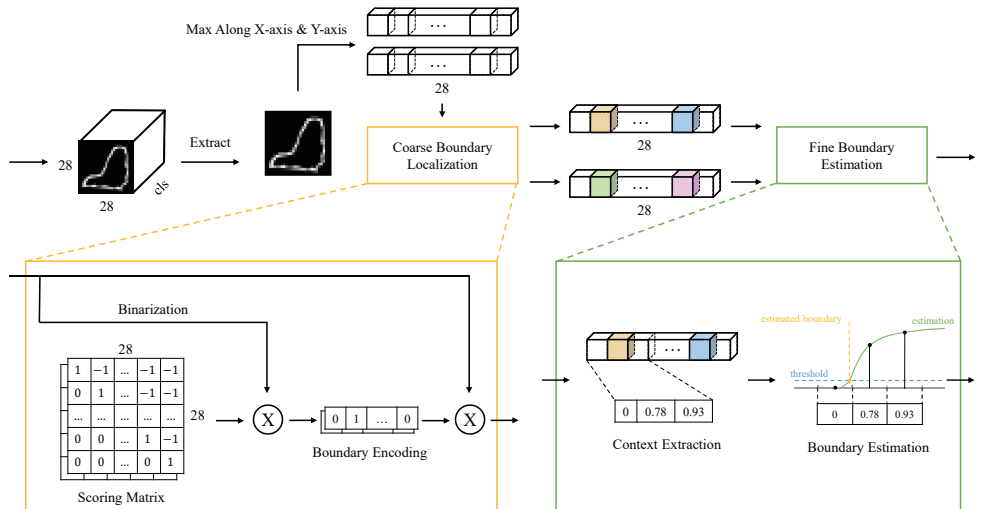


Figure 4: Illustration of part of the boundary estimation and box refinement module. Single-channel boundary possibility map is extracted based on the classification result and compressed into vectors along the x-axis and the y-axis. These vectors are then used to locate the coarse boundary and estimate the fine boundary.

3.1 Bounding box representation

Precise localization aims at eliminating the error between prediction and ground truth. For manually annotating the ground truth box, the most efficient way is to align each side of the box to the object boundary individually. However, rather than adjusting the edges, detectors conventionally choose to predict the centers and sizes of bounding boxes.

As shown in Figure 1, the center-size tuning method is inherently difficult to adjust an edge alone. The vertical and horizontal edges of rectangle box (E_l, E_r, E_t, E_b) can be represented by a set of scalar (l, r, t, b) or the box center and size (x, y, w, h):

$$E_l = f_l(l) = g_l(x, w/2) \quad (1)$$

$$E_r = f_r(r) = g_r(x, w/2) \quad (2)$$

$$E_t = f_t(t) = g_t(y, h/2) \quad (3)$$

$$E_b = f_b(b) = g_b(y, h/2) \quad (4)$$

Each edge depends on both center and size of the box. As a result, it is harder to adjust a single edge by the size-center method. This dilemma is widespread in modern detectors,

whether they predict center and size directly or the offset from proposal to ground truth box. A similar idea for precise localization is also reflected in the corner representation method [23]. The top-left corner and the bottom-right corner can be regarded as the intersection of corresponding edges, *i.e.*, $C_{tl}(l, t)$ and $C_{br}(r, b)$.

3.2 Coarse boundary localization

As shown in Figure 3 and Figure 4, our method can be decomposed into a two-step scheme, coarse boundary localization, and fine boundary estimation. We first apply RoIAlign to obtain and resize features in the proposal area. The $14 \times 14 \times C$ ($C = 256$ in the experiment) bounding box features is then followed by four 3×3 conv layers with stride 1, a 2×2 deconv layer with stride 2, and a 1×1 conv to output the $28 \times 28 \times \text{cls}$ ($\text{cls} = 80$ in MS COCO dataset [25]) boundary possibility map. With the classification result of the previous detector, we extract single-channel possibility map of a certain class, then take the maximum value on each row and column to compress it into two vectors. These vectors are fed into the coarse boundary localization module later.

In the coarse boundary localization module, we first binarize the vector (we choose the binarization threshold of $1e-4$) and multiply it by a scoring matrix and its transposed matrix. For the scoring matrix M_s in Figure 4, the product with the binarized vector v_b is as follows:

$$\vec{v}_b \times M_s = [\vec{v}_b \vec{m}_{c1}, \dots, \vec{v}_b \vec{m}_{c28}] \quad (5)$$

And for each $\vec{v}_b \vec{m}_{ci}$, there is:

$$\vec{v}_b \vec{m}_{ci} = \begin{cases} 0, & i < i_{fp} \\ 1, & i = i_{fp} \\ 1 - k', & i_{fp} < i \leq i_{lp} \\ -k, & i > i_{lp} \end{cases} \quad (6)$$

i_{fp} and i_{lp} are the indices of the first and last positive element in the vector. k and k' are integers that satisfy $k, k' \in [0, 28]$. These matrixes are designed to find the coarse position of the left/top and right/bottom boundary in the possibility map. The product result is then activated by the ReLU function.

3.3 Fine boundary estimation

As shown in Figure 4, the fine boundary estimation module first extracts the coarse boundary context, then refines the bounding box based on the estimated fine boundary. Differ from the universal interpolation method, our estimation method focuses on the distribution of boundaries rather than estimating the value between known values. Specifically, this makes it possible to choose a reasonable low threshold (0 in experiments) to reduce the outward expansion of boundary from interpolation.

There are several crucial requirements in the process of boundary estimation. The boundary distribution function $f_B : [0, 1] \rightarrow [0, 1]$ should be monotonically increasing and derivable. Besides, the gradient of the function should be smooth to reduce the exploding problem, *e.g.*, $f(x) = \sqrt{x}$ is untrainable as a distribution function because $f'(x)$ will explode when x approaches 0.

4 Experiments

4.1 Evaluation

We demonstrate the evaluation results of our proposed estimation method. These networks are trained and evaluated on the MS COCO dataset [25]. We follow the universal splitting method to train, validate and test our model on the COCO dataset. Detection results are evaluated with the standard COCO-style AP metric.

Method	Backbone	AP	AP ₅₀	AP ₇₅	AP _S	AP _M	AP _L
SSD513 [11, 28]	ResNet-101	31.2	50.4	33.3	10.2	34.5	49.8
YOLOv3-608 [33]	Darknet-53	33.0	57.9	34.4	18.3	35.4	41.9
Faster R-CNN [34]	ResNet-101-FPN	37.3	59.6	40.3	19.8	40.2	48.8
RetinaNet [26]	ResNet-101-FPN	39.1	59.1	42.3	21.8	42.7	50.2
Mask R-CNN [16]	ResNet-101-FPN	38.2	60.3	41.7	20.1	41.1	50.2
RetinaMask [10]	ResNet-50-FPN	39.4	58.6	42.3	21.9	42.0	51.0
Mask R-CNN(baseline)	ResNet-50-FPN	37.6	59.0	40.9	21.5	40.1	46.9
Ours	ResNet-50-FPN	39.6	59.4	42.5	22.2	42.2	49.8

Table 1: Comparison with state-of-the-art methods on COCO *test-dev* dataset. Our model achieves 2.0 overall AP improvement compared to the baseline model (Mask R-CNN with ResNet-50-FPN backbone).

We select *Mask R-CNN* [16] as the baseline in experiments. The parameters of the mask head in *Mask R-CNN* is used to initialize the network mentioned in Section 3.2 since the mask head has an inherent advantage to predict the boundary possibility map. We notice that most of the elements inside the object are similar (close to 1), which makes it meaningless to involve them in estimation. As a result, we implement a functional estimation $f(x)$ with the value x at the coarse boundary as the variable.

As shown in Table 1, we make improvements in overall AP and all individual AP metrics on the ResNet-50-FPN baseline with linear estimation $f(x) = x$. It also outperforms the baseline with a deeper ResNet-101-FPN backbone, which introduces much more computational cost.

4.2 Additional Experiments and Analysis

Comparison between different estimation functions. To survey the effect of different boundary distribution functions, we design three cases for comparative experiments. *Linear*, *exponential*, and *logarithmic* in Table 2 represent three functions of $f(x) = x$, $f(x) = x^2$, and $f(x) = \ln((e-1)x+1)$ respectively. In the experiment, we notice that the linear method

Method	AP	AP ₅₀	AP ₇₅	AP _S	AP _M	AP _L
Mask R-CNN	37.5	58.6	40.8	21.8	41.0	48.9
+ linear estimation	39.5	59.0	42.4	22.4	43.0	52.0
+ exponential estimation	39.3	58.9	41.9	22.4	42.9	51.7
+ logarithmic estimation	39.4	59.2	42.6	22.8	43.0	51.9

Table 2: Comparison with different estimation functions on COCO *val* dataset.

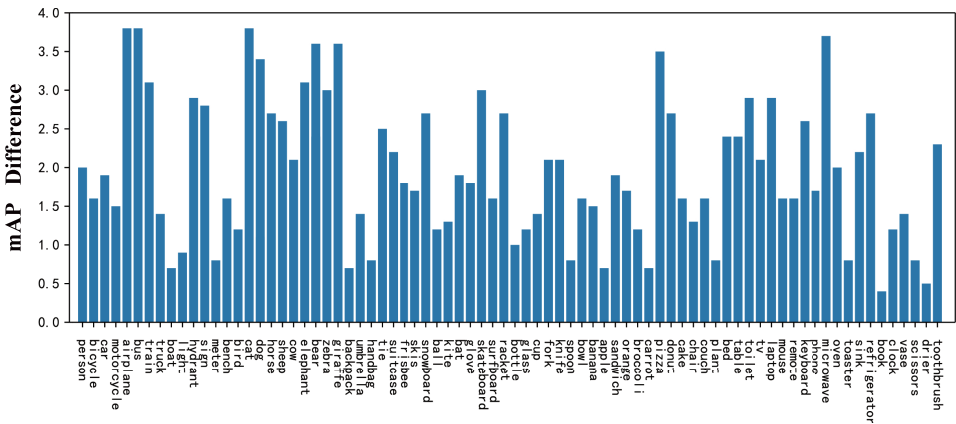


Figure 5: The mAP difference between our method and the baseline method on the COCO test-dev dataset for each category.

achieves better overall performance, specifically on large objects. The convex logarithmic function outperforms on smaller objects and has higher AP_{50} and AP_{75} , while the concave exponential function has no significant advantages.

Method	AP	AP_{50}	AP_{75}	AP_S	AP_M	AP_L
Mask R-CNN	37.5	58.6	40.8	21.8	41.0	48.9
w/o param init	38.5	58.3	41.1	21.6	42.3	50.5
w/ param init	39.5	59.0	42.4	22.4	43.0	52.0

Table 3: Comparison with different estimation functions on COCO *val* dataset.

Ablation study on extra annotation. Although no annotation data is used during training, it still introduces extra mask information when initializing the boundary prediction network with parameters in *Mask R-CNN* [16]. In order to ablate the influence of mask annotation, we deploy our method on *Faster R-CNN* [34] framework with randomly initialized parameters. As shown in Table 3, Our method remains effective with an improvement of 1.8% AP where little decline happens. Experiment results show that extra annotation such as mask is useful but not essential for the proposed method.

Method	AP	AP ₅₀	AP ₇₅	AP _S	AP _M	AP _L
Mask R-CNN	37.5	58.6	40.8	21.8	41.0	48.9
+ regression	38.7	58.1	41.5	21.9	42.2	51.2
+ edge refinement	39.5	59.0	42.4	22.4	43.0	52.0

Table 4: Comparison with common center-size representation and regression method on COCO *val* dataset.

Comparison with extra regression. Cascading methods are proven to be competent for precise localization [8]. To illustrate the superiority of boundary estimation, we compare our method to baseline methods with an extra regression stage. As shown in Table 4, our approach remains ahead of *Mask R-CNN* baselines, leading by up to 0.8% overall AP.

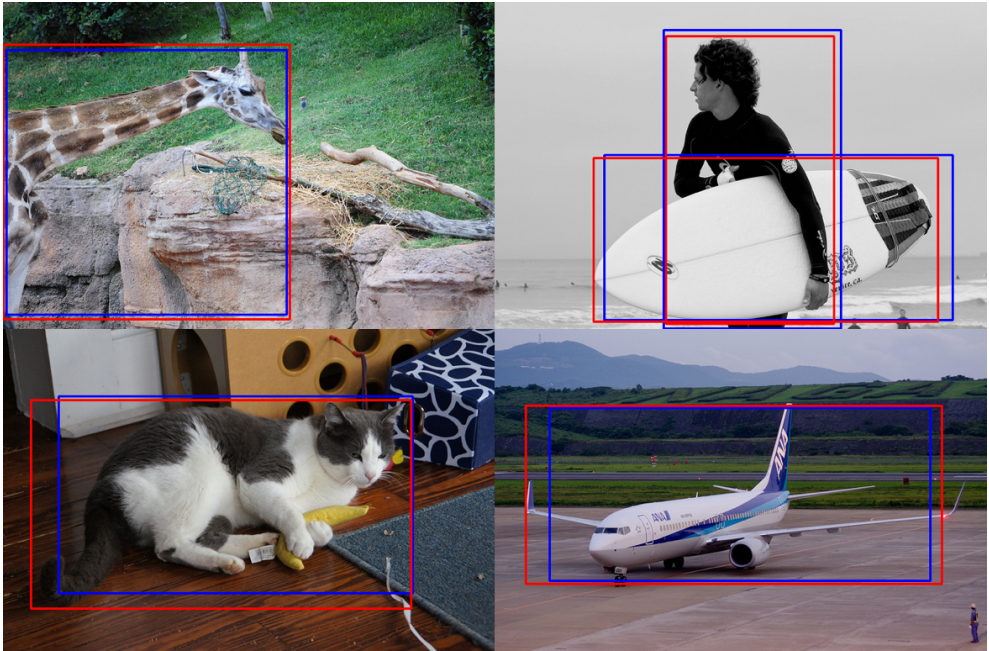


Figure 6: Detection results on the MS COCO *test-dev* dataset, with baseline model (blue) and our model (red).

5 Conclusion

In this work, we propose a novel method to detect objects precisely by estimating the boundary distribution of objects. We start with the aim of precise detection. Inspired by the manual annotation method, we leverage the advantage of the edge-focus box representation method. By predicting the coarse boundary and further estimating the fine boundary, our method is able to refine the edges of the bounding box based on previous localization results. Experimental results on the MS COCO dataset have shown the potentiality of our boundary estimation method on various detection pipelines without extra annotation.

References

- [1] P Arbeláez, M Maire, C Fowlkes, and J Malik. Contour detection and hierarchical image segmentation. *IEEE Transactions on Pattern Analysis and Machine Intelligence*, 33(5):898–916, 2011.
- [2] Gedas Bertasius, Jianbo Shi, and Lorenzo Torresani. Deepedge: A multi-scale bifurcated deep network for top-down contour detection. In *2015 IEEE Conference on Computer Vision and Pattern Recognition (CVPR)*, pages 4380–4389, 2015.
- [3] Z. Cai and N. Vasconcelos. Cascade r-cnn: High quality object detection and instance segmentation. *IEEE Transactions on Pattern Analysis and Machine Intelligence*, pages 1–1, 2019. doi: 10.1109/TPAMI.2019.2956516.

- [4] John Canny. A computational approach to edge detection. *IEEE Transactions on Pattern Analysis and Machine Intelligence*, 8(6):679–698, 1986.
- [5] Kai Chen, Wanli Ouyang, Chen Change Loy, Dahua Lin, Jiangmiao Pang, Jiaqi Wang, Yu Xiong, Xiaoxiao Li, Shuyang Sun, Wansen Feng, Ziwei Liu, and Jianping Shi. Hybrid task cascade for instance segmentation. In *2019 IEEE/CVF Conference on Computer Vision and Pattern Recognition (CVPR)*, pages 4974–4983, 2019.
- [6] Liang-Chieh Chen, Alexander Hermans, George Papandreou, Florian Schroff, Peng Wang, and Hartwig Adam. Masklab: Instance segmentation by refining object detection with semantic and direction features. In *2018 IEEE/CVF Conference on Computer Vision and Pattern Recognition*, pages 4013–4022, 2018.
- [7] J. Dai, H. Qi, Y. Xiong, Y. Li, G. Zhang, H. Hu, and Y. Wei. Deformable convolutional networks. In *2017 IEEE International Conference on Computer Vision (ICCV)*, pages 764–773, 2017. doi: 10.1109/ICCV.2017.89.
- [8] P. Dollár, Zhuowen Tu, and S. Belongie. Supervised learning of edges and object boundaries. In *2006 IEEE Computer Society Conference on Computer Vision and Pattern Recognition (CVPR'06)*, volume 2, pages 1964–1971, 2006.
- [9] Piotr Dollár and C. Lawrence Zitnick. Fast edge detection using structured forests. *IEEE Transactions on Pattern Analysis and Machine Intelligence*, 37(8):1558–1570, 2015.
- [10] Cheng-Yang Fu, Wei Liu, Ananth Ranga, Ambrish Tyagi, and Alexander C. Berg. Dssd : Deconvolutional single shot detector. *arXiv preprint arXiv:1701.06659*, 2017.
- [11] Cheng-Yang Fu, Mykhailo Shvets, and Alexander C. Berg. Retinamask: Learning to predict masks improves state-of-the-art single-shot detection for free. *arXiv: Computer Vision and Pattern Recognition*, 2019.
- [12] Yaroslav Ganin and Victor S. Lempitsky. N^4 -fields: Neural network nearest neighbor fields for image transforms. In *Asian Conference on Computer Vision*, pages 536–551, 2014.
- [13] R. Girshick. Fast r-cnn. In *2015 IEEE International Conference on Computer Vision (ICCV)*, pages 1440–1448, 2015. doi: 10.1109/ICCV.2015.169.
- [14] R. Girshick, J. Donahue, T. Darrell, and J. Malik. Rich feature hierarchies for accurate object detection and semantic segmentation. In *2014 IEEE Conference on Computer Vision and Pattern Recognition*, pages 580–587, 2014. doi: 10.1109/CVPR.2014.81.
- [15] K. He, X. Zhang, S. Ren, and J. Sun. Deep residual learning for image recognition. In *2016 IEEE Conference on Computer Vision and Pattern Recognition (CVPR)*, pages 770–778, Los Alamitos, CA, USA, jun 2016. IEEE Computer Society. doi: 10.1109/CVPR.2016.90. URL <https://doi.ieeecomputersociety.org/10.1109/CVPR.2016.90>.
- [16] K. He, G. Gkioxari, P. Dollár, and R. Girshick. Mask r-cnn. *IEEE Transactions on Pattern Analysis and Machine Intelligence*, 42(2):386–397, 2020. doi: 10.1109/TPAMI.2018.2844175.

- [17] Zhaojin Huang, Lichao Huang, Yongchao Gong, Chang Huang, and Xinggang Wang. Mask scoring r-cnn. In *2019 IEEE/CVF Conference on Computer Vision and Pattern Recognition (CVPR)*, pages 6409–6418, 2019.
- [18] Jyh-Jing Hwang and Tyng-Luh Liu. Pixel-wise deep learning for contour detection. In *ICLR (Workshop)*, 2015.
- [19] Yonghyun Kim, Taewook Kim, Bong-Nam Kang, Jieun Kim, and Daijin Kim. Ban: Focusing on boundary context for object detection. In C.V. Jawahar, Hongdong Li, Greg Mori, and Konrad Schindler, editors, *Computer Vision – ACCV 2018*, pages 555–570, Cham, 2019. Springer International Publishing. ISBN 978-3-030-20876-9.
- [20] Josef Kittler. On the accuracy of the sobel edge detector. *Image and Vision Computing*, 1(1):37–42, 1983.
- [21] S. Konishi, A.L. Yuille, J.M. Coughlan, and Song Chun Zhu. Statistical edge detection: learning and evaluating edge cues. *IEEE Transactions on Pattern Analysis and Machine Intelligence*, 25(1):57–74, 2003.
- [22] Alex Krizhevsky. Learning multiple layers of features from tiny images. Technical report, 2009.
- [23] Hei Law and Jia Deng. Cornernet: Detecting objects as paired keypoints. *International Journal of Computer Vision*, 128(3):642–656, Mar 2020. ISSN 1573-1405. doi: 10.1007/s11263-019-01204-1. URL <https://doi.org/10.1007/s11263-019-01204-1>.
- [24] Joseph J. Lim, C. Lawrence Zitnick, and Piotr Dollár. Sketch tokens: A learned mid-level representation for contour and object detection. In *2013 IEEE Conference on Computer Vision and Pattern Recognition*, pages 3158–3165, 2013.
- [25] Tsung-Yi Lin, Michael Maire, Serge Belongie, James Hays, Pietro Perona, Deva Ramanan, Piotr Dollár, and C. Lawrence Zitnick. Microsoft coco: Common objects in context. In David Fleet, Tomas Pajdla, Bernt Schiele, and Tinne Tuytelaars, editors, *Computer Vision – ECCV 2014*, pages 740–755, Cham, 2014. Springer International Publishing. ISBN 978-3-319-10602-1.
- [26] Tsung-Yi Lin, Priya Goyal, Ross B. Girshick, Kaiming He, and Piotr Dollár. Focal loss for dense object detection. *2017 IEEE International Conference on Computer Vision (ICCV)*, pages 2999–3007, 2017.
- [27] Shu Liu, Lu Qi, Haifang Qin, Jianping Shi, and Jiaya Jia. Path aggregation network for instance segmentation. In *2018 IEEE/CVF Conference on Computer Vision and Pattern Recognition*, pages 8759–8768, 2018.
- [28] Wei Liu, Dragomir Anguelov, Dumitru Erhan, Christian Szegedy, Scott Reed, Cheng-Yang Fu, and Alexander C. Berg. Ssd: Single shot multibox detector. In Bastian Leibe, Jiri Matas, Nicu Sebe, and Max Welling, editors, *Computer Vision – ECCV 2016*, pages 21–37, Cham, 2016. Springer International Publishing. ISBN 978-3-319-46448-0.
- [29] X. Lu, B. Li, Y. Yue, Q. Li, and J. Yan. Grid r-cnn. In *2019 IEEE/CVF Conference on Computer Vision and Pattern Recognition (CVPR)*, pages 7355–7364, 2019. doi: 10.1109/CVPR.2019.00754.

- [30] D. Marr and E. Hildreth. Theory of edge detection. *Proceedings of The Royal Society B: Biological Sciences*, 207(1167):187–217, 1980.
- [31] D.R. Martin, C.C. Fowlkes, and J. Malik. Learning to detect natural image boundaries using local brightness, color, and texture cues. *IEEE Transactions on Pattern Analysis and Machine Intelligence*, 26(5):530–549, 2004.
- [32] J. Redmon, S. Divvala, R. Girshick, and A. Farhadi. You only look once: Unified, real-time object detection. In *2016 IEEE Conference on Computer Vision and Pattern Recognition (CVPR)*, pages 779–788, 2016. doi: 10.1109/CVPR.2016.91.
- [33] Joseph Redmon and Ali Farhadi. Yolov3: An incremental improvement. *arXiv: Computer Vision and Pattern Recognition*, 2018.
- [34] S. Ren, K. He, R. Girshick, and J. Sun. Faster r-cnn: Towards real-time object detection with region proposal networks. *IEEE Transactions on Pattern Analysis and Machine Intelligence*, 39(6):1137–1149, 2017. doi: 10.1109/TPAMI.2016.2577031.
- [35] Xiaofeng Ren. Multi-scale improves boundary detection in natural images. In *ECCV '08 Proceedings of the 10th European Conference on Computer Vision: Part III*, pages 533–545, 2008.
- [36] Olga Russakovsky, Jia Deng, Hao Su, Jonathan Krause, Sanjeev Satheesh, Sean Ma, Zhiheng Huang, Andrej Karpathy, Aditya Khosla, and Michael Bernstein. Imagenet large scale visual recognition challenge. *International Journal of Computer Vision*, 115(3):211–252, 2015.
- [37] Wei Shen, Xinggang Wang, Yan Wang, Xiang Bai, and Zhijiang Zhang. Deepcontour: A deep convolutional feature learned by positive-sharing loss for contour detection. In *2015 IEEE Conference on Computer Vision and Pattern Recognition (CVPR)*, pages 3982–3991, 2015.
- [38] Karen Simonyan and Andrew Zisserman. Very deep convolutional networks for large-scale image recognition. *Computer ence*, 2014.
- [39] C. Szegedy, Wei Liu, Yangqing Jia, P. Sermanet, S. Reed, D. Anguelov, D. Erhan, V. Vanhoucke, and A. Rabinovich. Going deeper with convolutions. In *2015 IEEE Conference on Computer Vision and Pattern Recognition (CVPR)*, pages 1–9, 2015. doi: 10.1109/CVPR.2015.7298594.
- [40] Z. Tian, C. Shen, H. Chen, and T. He. Fcos: Fully convolutional one-stage object detection. In *2019 IEEE/CVF International Conference on Computer Vision (ICCV)*, pages 9626–9635, 2019. doi: 10.1109/ICCV.2019.00972.
- [41] Vincent Torre and Tomaso A. Poggio. On edge detection. *IEEE Transactions on Pattern Analysis and Machine Intelligence*, 8(2):147–163, 1986.
- [42] Jiaqi Wang, Wenwei Zhang, Yuhang Cao, Kai Chen, Jiangmiao Pang, Tao Gong, Jianping Shi, Chen Change Loy, and Dahua Lin. Side-aware boundary localization for more precise object detection, 2020.
- [43] Saining Xie and Zhuowen Tu. Holistically-nested edge detection. *International Journal of Computer Vision*, 125(1):3–18, 2017.

- [44] Xingyi Zhou, Dequan Wang, and Philipp Krähenbühl. Objects as points. *CoRR*, abs/1904.07850, 2019. URL <http://arxiv.org/abs/1904.07850>.
- [45] C. Lawrence Zitnick and Piotr Dollár. Edge boxes: Locating object proposals from edges. In David Fleet, Tomas Pajdla, Bernt Schiele, and Tinne Tuytelaars, editors, *Computer Vision – ECCV 2014*, pages 391–405, Cham, 2014. Springer International Publishing. ISBN 978-3-319-10602-1.